Surface-induced dissociation of singly and multiply protonated polypropylenamine dendrimers

ARTICLE *in* JOURNAL OF THE AMERICAN SOCIETY FOR MASS SPECTROMETRY · JUNE 1999

Impact Factor: 2.95 · DOI: 10.1016/S1044-0305(99)00008-2 · Source: PubMed

6 AUTHORS, INCLUDING:

Adriana Gielbert
Animal and Plant Health Agency
22 PUBLICATIONS **3,417** CITATIONS
SEE PROFILE

Arpad A Somogyi
The Ohio State University
123 PUBLICATIONS **3,495** CITATIONS
SEE PROFILE

Surface-Induced Dissociation of Singly and Multiply Protonated Polypropylenamine Dendrimers

Janine de Maaijer-Gielbert
FOM-institute for Atomic and Molecular Physics, Kruislaan, SJ Amsterdam, The Netherlands

Chungang Gu, Árpád Somogyi, and Vicki H. Wysocki
Department of Chemistry, University of Arizona, Tucson, Arizona, USA

Piet G. Kistemaker and Tina L. Weeding
FOM-institute for Atomic and Molecular Physics, Kruislaan, SJ Amsterdam, The Netherlands

The ease of fragmentation of various charge states of protonated polypropylenamine (POPAM) dendrimers is investigated by surface-induced dissociation. Investigated are the protonated diaminobutane propylenamines [DAB(PA)$_n$] DAB(PA)$_8$ (1+ and 2+), DAB(PA)$_{16}$ (2+ and 3+), and DAB(PA)$_{32}$ (3+ and 4+). These ions have been proposed to fragment by charge-directed intramolecular nucleophilic substitution (S_Ni) reactions. Differences in relative fragment ion abundances between charge states can be related to the occupation of different protonation sites. These positions can be rationalized based on estimates of Coulomb energies and gas-phase basicities of the protonation/fragmentation sites. The laboratory collision energies at which the fragment ion current is ~50% of the total ion current were found to increase with the size, but to be independent of charge state of the protonated POPAM dendrimers. It is suggested that intramolecular Coulomb repulsion within the multiply protonated POPAM dendrimers selected for activation does not readily result in easier fragmentation, which is in accordance with the proposed fragmentation mechanism. (J Am Soc Mass Spectrom 1999, 10, 414–422) © 1999 American Society for Mass Spectrometry

The introduction of electrospray ionization (ESI) [1, 2] has greatly facilitated the production of multiply charged ions. ESI has made it possible to analyze high molecular weight compounds, provided they can carry the required number of charges, in a m/z range accessible with most mass analyzers. Tandem mass spectrometry (MS/MS) has been applied successfully for increasingly large systems. Most of the MS/MS investigations concerning multiply charged ions have focused on protonated peptides or small proteins. For example, complete sequencing of multiply charged biopolymers <3 ku has been demonstrated [3, 4], whereas sequence information has also been obtained for larger biopolymers such as carbonic anhydrase (29 ku) [5] and serum albumins (66 ku) [6]. An important aspect of the dissociation of multiply protonated ions is the often observed easier fragmentation with increasing charge state [3]. This is favorable for example when the MS/MS setup is limited to low-energy collisional activation [3, 7]. In many studies, the influence of peptide composition and charge state on the ease of fragmentation have been investigated [4, 7–14]. In most of these studies either gas-phase collision-induced dissociation (CID) [4, 8–10, 15] or surface-induced dissociation (SID) [11–14] were employed, and the peptide results from both indicate that fragmentation is often facilitated for a higher charge state. An exception is reported by Jockush et al. who determined an increase in the fragmentation energy of ubiquitin 6+ to 11+ in black-body infrared dissociation experiments. The authors propose that the influence of multiple charges in ubiquitin is by changing the ion conformation and/or charge distribution rather than by lowering bond dissociation energies [16].

Several authors have proposed an explanation for the easier fragmentation of multiply charged peptides. Gaskell and co-workers use the term "increased charge heterogeneity" [9, 17]. Wysocki and co-workers have proposed the "mobile-proton" model [12–14]. The similar models state that factors that allow protons to access less basic sites in the molecules lead to enhanced nonselective cleavage that provides sequence information. The participation of amide nitrogens, which have a relatively low gas-phase basicity within the peptide, in the protonation is assumed to be required to initiate the

Address reprint requests to Piet G. Kistemaker, FOM-institute for Atomic and Molecular Physics, Kruislaan 407, 1098 SJ Amsterdam, The Netherlands.

1044-0305/99/$20.00
PII S1044-0305(99)00008-2

Received September 2, 1998
Revised January 4, 1999
Accepted January 4, 1999

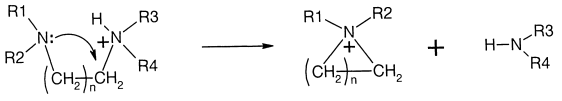

Scheme 1

relatively low-energy charge-directed fragmentations [18–20]. Although proton migration to the less basic amide nitrogen is an endothermic process, the significant weakening of the amide bonds in these forms "drives" the amide bond cleavages faster than in other protonated forms [18, 19]. Separate from these explanations, multiply charged ions have also been proposed to be inherently less stable than singly charged ions [21, 22]. Rockwood et al. predict a lower activation energy for dissociation of a linear polymer with higher charge state, as a result of the Coulomb interactions [21]. Vékey and Gömöry have calculated potential energy profiles using semiempirical and ab initio methods for doubly protonated tetraglycine and conclude that the presence of multiple charge sites in a peptide may lead to further weakening of the amide bond [22]. However, this result has not been verified experimentally, because a doubly protonated ion is not obtained in an ESI source for such a small nonbasic peptide.

To further study the charge-state dependence of the fragmentation efficiencies, we have looked for compounds which can be multiply protonated, but in which the gas-phase basicity of various sites in the molecule does not vary as greatly as in peptides. In the present work the size and charge state dependence of the fragmentation efficiency of protonated POPAM dendrimers $DAB(PA)_8$, $DAB(PA)_{16}$, and $DAB(PA)_{32}$ is investigated. These dendrimers consist of a 1,4-diaminobutane (DAB) core group in which the amine hydrogens have been replaced by propylenamine (PA) groups. Therefore, they contain tertiary amine "inner" nitrogens and primary amine end groups [23]. The presence of many amine nitrogens in a POPAM dendrimer makes internal solvation possible, resulting in a high gas-phase basicity. In general, a protonation site in a polyamine compound is assumed to consist of several amine nitrogens to which the proton is hydrogen bound. Experimental data by Yamdagni and Kebarle indicate that proton-bound cyclic structures are formed in singly protonated polyamines [24].

The proposed fragmentation mechanism for polytertiary alkylamines is a charge-directed intramolecular nucleophilic substitution (S_Ni) [25]. A generalization of the S_Ni fragmentation mechanism for these compounds, based on earlier publications for singly protonated POPAM dendrimers [26, 27], is shown in Scheme **1**. In the POPAM dendrimers the protonation of the sites which have the highest gas-phase basicity within the molecule, the tertiary amine nitrogens, can give rise to the S_Ni fragmentation reactions, and therefore prior mobilization of the proton is not necessary. This is different from the situation in peptides, where the proton may reside at a basic site where it can not readily initiate fragmentation, e.g., at the side chain of a basic amino acid residue or a free N-terminal amino group. In protonated dendrimers, the activation energies for the S_Ni reactions may not differ significantly and do not depend significantly on the protonation site. A nucleophilic attack by a nonprotonated amine nitrogen is required: the proton primarily determines the preferred position of the attack but not the bond dissociation energy of the C–N bonds. For protonated peptides, the activation energy for fragmentation is determined by both the activation energy for intramolecular proton transfer and the C–N bond dissociation energy. In this case the addition of a second proton has a pronounced effect [13] besides possible Coulomb destabilization.

SID, pioneered by Cooks and co-workers [28], has proved to be a valuable tool in the energy-resolved fragmentation of many different compounds [12, 28]. With SID up to 30% of the laboratory collision energy (kinetic energy) can be converted into internal energy of the projectile ions, and the energy deposition efficiency is shown to be approximately constant up to 80 eV collision energy [29, 30]. The SID studies on the effects of peptide composition and charge state utilize fragmentation efficiency curves, which relate the percent fragmentation to the laboratory collision energy. For a peptide with a given amino acid sequence, lower characteristic fragmentation energies (E_{chr}) have been observed for the multiply protonated species [13]. E_{chr} is defined as the laboratory collision energy at the inflection point of the fragmentation efficiency curve.

In the first part of this article we present the ESI/SID spectra for various charge states of the dendrimers. In the second part we present SID fragmentation efficiency curves of protonated dendrimers to demonstrate the effects of size and charge state on the ease of fragmentation.

Experimental

The ESI/SID experiments have been performed in a tandem quadrupole instrument which has been described in detail earlier [31], and is based on an instrument designed by Cooks and co-workers [32]. Briefly, it consists of two Extrel 4000 u quadrupoles (now ABB Extrel, Pittsburgh, PA) arranged in a 90° geometry with the SID surface positioned to intersect the ion optical path of each quadrupole. The angles between the incoming or outgoing ion beams and the surface normal are 45 ± 5°. Ions are produced by ESI and introduced into vacuum via a stainless steel heated inlet capillary (about 400 K) which is positioned in front of a skimmer [33, 34].

In the ESI source, there is a 30 V difference between the capillary and the skimmer to improve ion extraction; this difference is maintained for all mass spectrometry and MS/MS experiments and results in a relatively low level of excitation of the ions prior to the surface collision [11]. The SID collision energy is defined by the voltage difference between the skimmer and the collision surface multiplied by the charge state of the ion.

The skimmer potential was kept constant at 90 V and the surface potential was varied [e.g., 40 V applied to the surface for a doubly charged ion gives $2e \times (90 - 40)$ V = 100 eV collision energy]. The parent ions are selected by the first quadrupole, and after the collision with the surface the fragment ions are analyzed by scanning the second quadrupole. We utilized a self-assembled monolayer (SAM) of fluoroalkanethiols on a gold surface, i.e., CF_3–$(CF_2)_7$–$(CH_2)_2$–S–Au (hereafter, referred to as FC_{10} surface) for all SID spectra reported in this paper. To maximize sensitivity, the quadrupole mass analyzers are routinely set to a resolution of 3–5 mass units (FWHH). Some experiments have been performed with unit resolution to confirm the accuracy of peak assignment.

The dendrimers $DAB(PA)_8$, $DAB(PA)_{16}$, and $DAB(PA)_{32}$ have been obtained from DSM (Geleen, The Netherlands). For ESI, 75–150 μM solutions in a 3:1 methanol:water mixture are used. To enhance multiple protonation, acetic acid is added to a concentration between 0.1% and 2%, to optimize the intensity of a specific charge state to be selected for SID.

Results and Discussion

SID Spectra

Figure 1a shows the SID spectrum resulting from 45 eV collisions of singly charged $DAB(PA)_8H^+$ ions with the FC_{10} surface. The formation of most fragments, such as m/z 58, 172, 243, 414, and 642, can be explained by the S_Ni reactions shown in Schemes **2** and **3**. In the 45 eV SID spectrum, m/z 172 is the base peak. The fragment at m/z 414 has been identified as the lowest-energy fragmentation channel, and m/z 172 to the next lowest, by both thermal decomposition experiments and low energy CID experiments in an ion trap mass spectrometer [35]. The possibility of sequential fragmentation, such as the formation of m/z 172 out of m/z 414 (see Scheme **2**), has been confirmed by CID MS^3 experiments in an ion trap mass spectrometer [35] and in a triple quadrupole mass spectrometer [26]. The abundance of the fragment at m/z 58 is low in Figure 1a but it increases with increasing collision energy. At collision energies higher than 100 eV the spectrum is dominated by m/z 58. The fragment at m/z 642 is of low intensity at all collision energies utilized with a maximum (10% of the base peak) around 30–35 eV collision energy (not shown). Other minor fragments in the 45 eV SID spectrum of $DAB(PA)_8H^+$ are observed at m/z 70, 72, 84, 101, 112, 115, 144, and 243 (unit resolution experiments). These can be explained by sequential S_Ni rearrangement reactions in the ion, terminated by a S_Ni fragmentation. Examples are shown in Scheme **3** for formation of the fragments m/z 115 and 243.

Figure 1b shows a 45 eV SID spectrum obtained by collision of doubly charged $DAB(PA)_8H_2^{2+}$ with a FC_{10} surface. The base peak is the precursor (doubly charged) ion. The ratio of the total fragment ion current

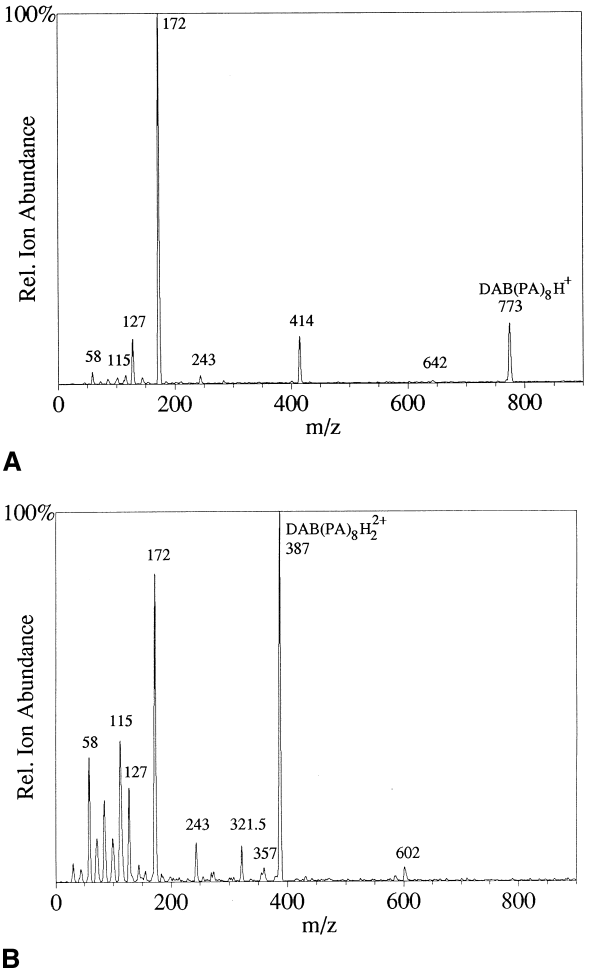

Figure 1. 45 eV SID spectrum upon collision with a FC_{10} surface of (**a**) $DAB(PA)_8H^+$ and (**b**) $DAB(PA)_8H_2^{2+}$. In (**b**), a blowup of the region $> m/z$ 400 does not reveal any peaks with $s/n > 3$ other than m/z 602.

to the total ion current is the same for the spectra in Figure 1a, b. This indicates that at the collision energy of 45 eV, the doubly charged ion is not more fragile than the singly charged one. The ease of relative fragmenta-

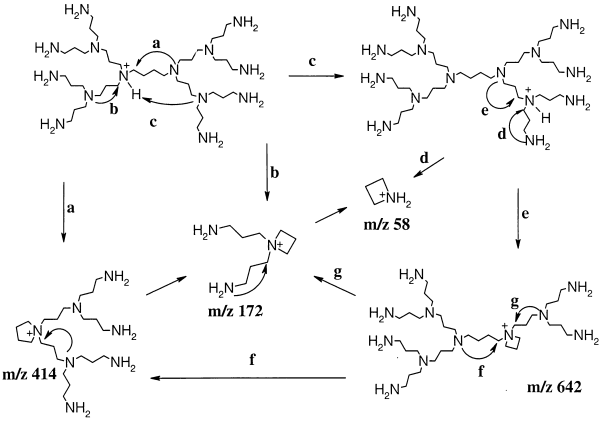

Scheme 2

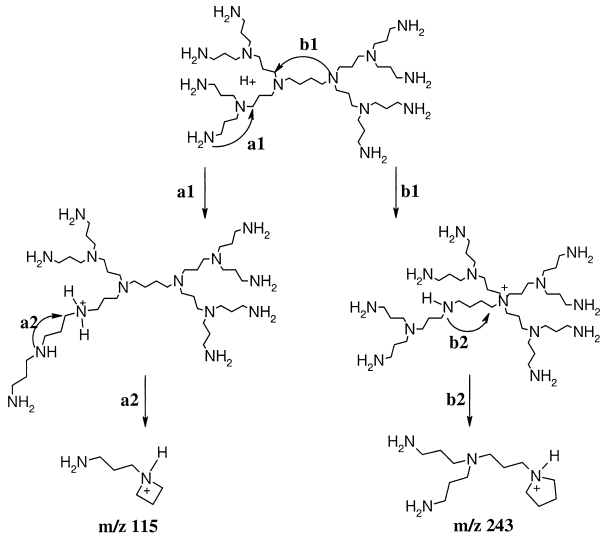

Scheme 3

tion of different charge states will be further discussed below. The most abundant fragment is again the ion at m/z 172, the complementary ion of which appears only as a minor peak in the spectrum at m/z 602. Fragments at lower masses, such as at m/z 127, 115, and 58, are more intense in the SID spectrum of the doubly charged ion than in that of the singly charged ion. This is attributed to the distribution of the protonation to different sites caused by Coulomb repulsion, and is discussed in the following section. Scheme **4** shows a proposal for the S_Ni reactions leading to the fragments observed for $DAB(PA)_8H_2^{2+}$. Almost any structure in Scheme **4** can fragment further into m/z 172 and 58.

In the SID spectra of triply charged $DAB(PA)_8H_3^{3+}$ the abundance of m/z 58 is higher than that of m/z 172 at all SID collision energies investigated. This indicates that the S_Ni reactions involving the outer groups are relatively facilitated (see discussion below).

Figure 2a shows the 90 eV SID spectrum of doubly charged $DAB(PA)_{16}H_2^{2+}$ (m/z 844) on the FC_{10} surface. Below m/z 200 this spectrum shows the same fragments as observed for $DAB(PA)_8H_n^{n+}$ (n = 1, 2). The base peak corresponds again to the ion at m/z 172. Most fragments of $DAB(PA)_{16}H_2^{2+}$ can be explained based on the S_Ni fragmentation mechanism (Scheme **5**). We cannot provide a logical explanation for the abundant fragment at m/z 285 in the 90 eV SID spectrum of $DAB(PA)_{16}H_3^{3+}$ (m/z 563) (Figure 2b). The SID spectra of $DAB(PA)_{32}H_3^{3+}$ and $DAB(PA)_{32}H_4^{4+}$ (not shown) also show mostly S_Ni fragmentation products: for example complementary ion pairs such as m/z 58 and $[MH_n - 58]^{(n-1)+}$, m/z 172 and $[MH_n - 172]^{(n-1)+}$, m/z 400 and $[MH_n - 400]^{(n-1)+}$, and, upon loss of a 131 u neutral fragment, $[MH_n - 131]^{n+}$ (n = 3, 4).

Gas-Phase Basicity and Coulomb Interactions

As indicated in Scheme **2**, the formation of m/z 414 and 172 from $DAB(PA)_8H^+$ (Figure 1a, b) can follow upon protonation at either of the innermost tertiary amines (N-3 and N-3′) (see Scheme **6** for numerical designation of different amine nitrogens). The protonation at these inner tertiary nitrogens is favored by the relatively high proton affinity values of tertiary amines. Table 1 summarizes proton affinities for various diamines, which we consider to be representative for the amine groups in the POPAM dendrimers [36]. We assume that in $DAB(PA)_8H^+$ at low internal energy the proton is solvated between at least the two central tertiary nitrogens because these nitrogens have the largest substituents and therefore the highest gas-phase basicity. In addition, the resulting structure is a proton-bound

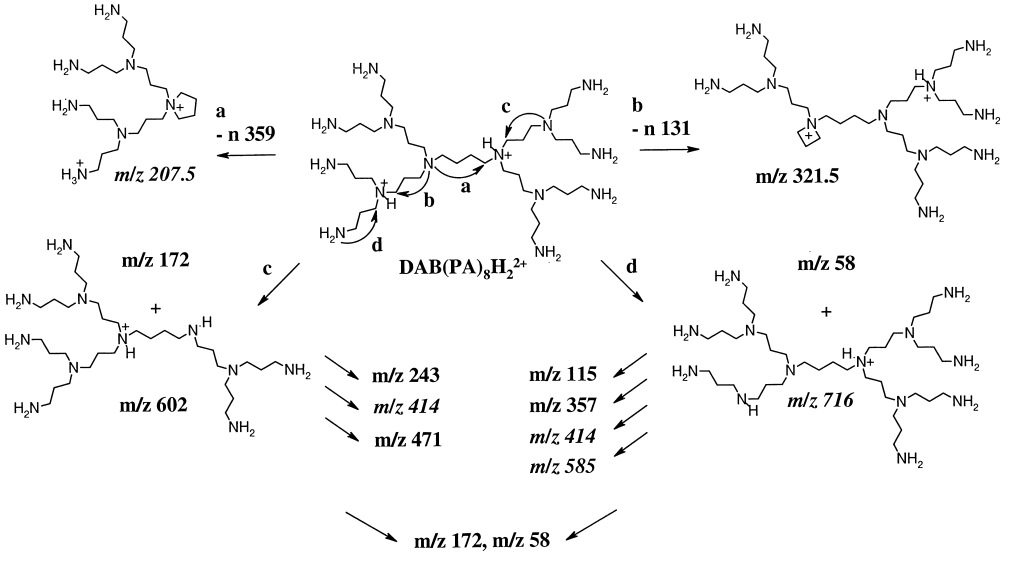

Scheme 4

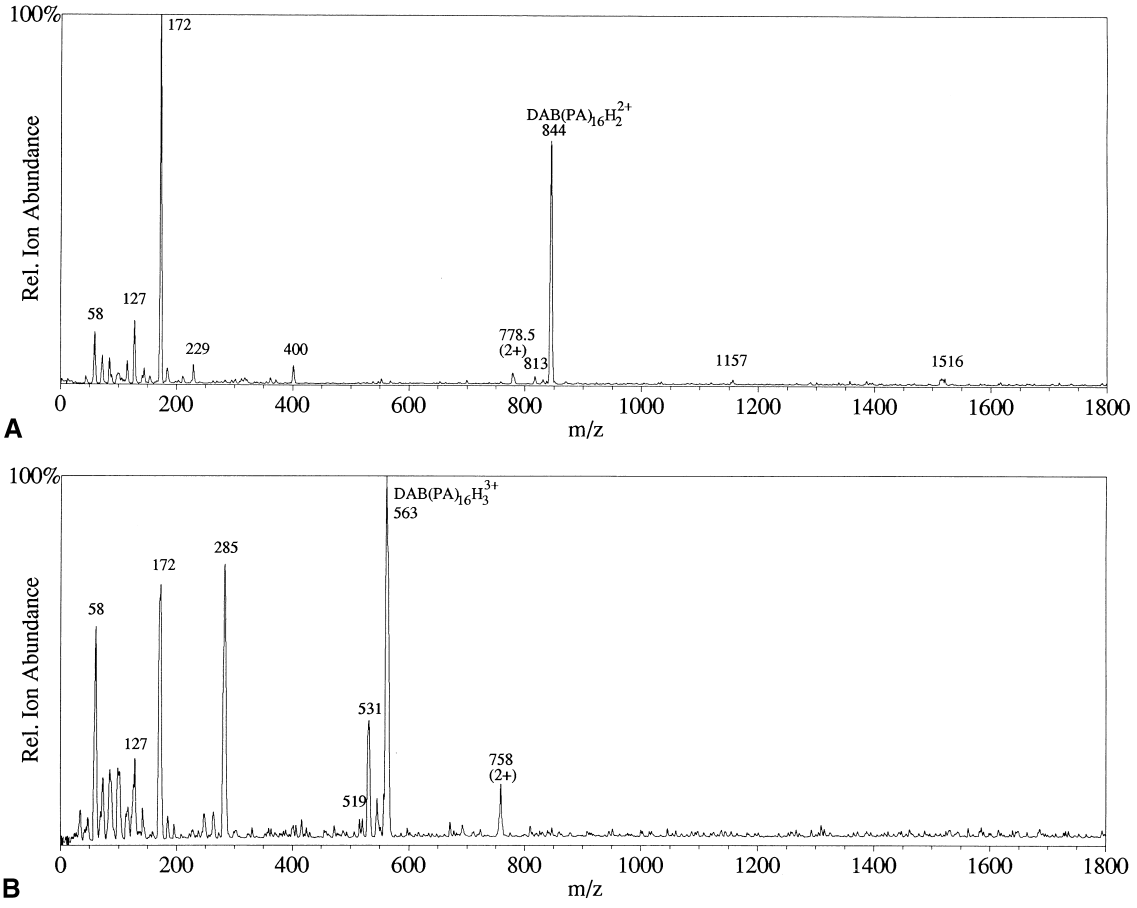

Figure 2. 90 eV SID spectrum upon collision with a FC_{10} surface of (**a**) $DAB(PA)_{16}H_2^{2+}$ and (**b**) $DAB(PA)_{16}H_3^{3+}$.

"cyclicized" diaminobutane, which has a relatively small ring strain enthalpy [37].

When the collision (internal) energy is increased, both fragmentation and transfer of the proton to sites with a lower proton affinity can take place. This can in turn lead to fragmentation reactions at different sites, by which the low-mass fragments such as m/z 58 and m/z 115 can be formed (see Schemes **2** and **3**).

In multiply protonated dendrimers the distribution of the charge sites is governed both by the gas-phase basicity of the site and by the Coulomb interactions of the charges in the ion. Schnier et al. have proposed that for a multiply protonated molecule, the lowest-energy configuration of the charges is such that the relative free energy of a given charge configuration is minimized [38]. This relative free energy is minimized when

$$\sum_{\substack{i,j \\ i>j}}^{n} \frac{q^2}{4\pi\epsilon_0\epsilon_r r_{ij}} - \sum_{i=n}^{n} \mathrm{GB}_i^{\mathrm{intr}} \qquad (1)$$

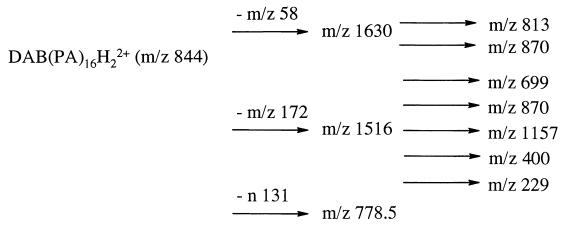

Scheme 5

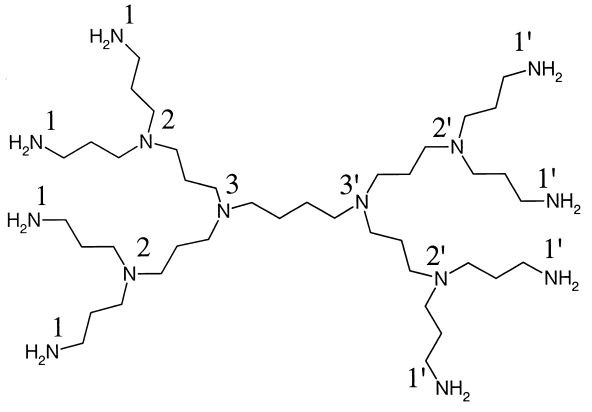

Scheme 6

Table 1. Gas-phase proton affinities of several primary and tertiary diamines, as obtained from [36]

Molecule	Proton affinity (kJ/mol)	Proton affinity (eV)
$NH_2(C_3H_6)NH_2$	979	10.1
$NH_2(C_4H_8)NH_2$	994	10.3
$NH_2(C_5H_{10})NH_2$	996	10.3
$NH_2(C_6H_{12})NH_2$	994.4	10.3
$(CH_3)_2N(C_3H_6)NH_2$	1006	10.4
$(CH_3)_2N(C_3H_6)N(CH_3)_2$	1017	10.5
$(CH_3)_2N(C_4H_8)N(CH_3)_2$	1029	10.7
$(CH_3)_2N(C_6H_{12})N(CH_3)_2$	1023	10.6

is minimized, where q is the charge, ϵ_0 is the vacuum permittivity, ϵ_r the relative permittivity of the medium, r_{ij} the distance between the charges, and GB_i^{intr} the intrinsic gas-phase basicity of a protonation site. This and related expressions have been helpful in predicting the maximum charge state and proton transfer reactivity of multiply protonated compounds [38, 39]. The relative free energies associated with the charge distribution in a multiply protonated dendrimer can in principle be determined from expression 1. It is clear that the Coulomb interactions decrease when the charge sites are more widely separated. Although the exact determination of the lowest-energy proton distribution is complicated by the absence of values for the gas-phase basicity of the protonation sites in the POPAM dendrimer and for the distances in the lowest-energy geometry, we can estimate the magnitude of these effects. For the Coulomb interactions in $DAB(PA)_8H_2^{2+}$ we assume that the maximum possible distance between the charges is realized when NH_2 groups on opposite sides of the dendrimer are protonated. Using C–C and C–N bond lengths of 1.54 and 1.47 Å, respectively, and assuming average bond angles of 110°, the distance is about 25 Å giving 0.6 eV Coulomb energy [using $E_{Coulomb}(eV) = 14.4/r(Å)$]. The displacement of one of the protons from the "outer" shell one layer inward (by one propyl group) leads to an increase in the Coulomb energy of 0.1–0.3 eV. The proton affinity of the tertiary amine nitrogens is higher than that of the primary nitrogens of the outer shells by 0.1–0.3 eV. Thus the changes in gas-phase basicity and Coulomb repulsion are comparable, such that a single lowest-energy proton distribution cannot be predicted. However, it is reasonable to say that for higher charge states there is increased participation of the outer amine nitrogens (N-2 and N-1 in Scheme **6**) in the solvation of the protons, compared to that for $DAB(PA)_8H^+$ where at low internal energy the proton is solvated by central tertiary nitrogens (N-3 and N-3′). This assumption is supported by the higher relative abundance of fragments from the periphery of the ion for higher charge states of the dendrimers (compare Figure 1a with 1b, and Figure 2a with 2b). However, the probability that two of the outer primary amines are simultaneously protonated in a doubly charged dendrimer is low. For example, proton transfer from sites N-2 and N-2′ to N-1 and N-1′ in $DAB(PA)_8H_2^{2+}$ decreases the Coulomb repulsion with only 0.3 eV, but the gas-phase basicity with 0.6 eV. Similarly, we assume that the probability of simultaneous protonation of inner nitrogens (N-3 and N-2 as well as N-3 and N-3′) is low because of strong Coulomb repulsion, as supported by the absence of m/z 414 from the SID spectra of $DAB(PA)_8H_2^{2+}$. Such fragments containing the 5-membered ring are also absent from the SID fragment spectra of the other multiply protonated dendrimers. For example, there is no peak at m/z 870 in the spectra of $DAB(PA)_{16}H_2^{2+}$, whereas it has been observed in the SID fragment spectra of the singly protonated form, $DAB(PA)_{16}H^+$.

Fragmentation Efficiency

Figure 3 shows the ESI/SID fragmentation efficiency curves obtained for $DAB(PA)_8H^+$, $DAB(PA)_8H_2^{2+}$, $DAB(PA)_{16}H_2^{2+}$, $DAB(PA)_{16}H_3^{3+}$, $DAB(PA)_{32}H_3^{3+}$, and $DAB(PA)_{32}H_4^{4+}$. The fragmentation efficiency curves clearly show the independence of the characteristic fragmentation energy E_{chr} on the dendrimer charge state and the increase of E_{chr} with dendrimer size. The obtained values of E_{chr} are given in Table 2, which also gives the number of degrees of freedom (DOF) for each of the ions. Previously an approximately linear correlation between the number of DOF and E_{chr} for a series of singly protonated oligopeptides has been suggested [13, 40]. However, for the dendrimers investigated in this study, we do not find a linear relationship between E_{chr} and DOF. The approximate doubling of E_{chr} of $DAB(PA)_{16}$ compared to E_{chr} of $DAB(PA)_8$ is not followed by another doubling of E_{chr} for $DAB(PA)_{32}$. Under assumption of statistical distribution of the internal energy on the time scale of the SID experiments, a possible explanation for this nonlinearity can be an influence of the size or shape of the parent ion on the energy deposition efficiency. This effect has been suggested by Beck et al. for fullerenes [41]. On the other hand, nonstatistical behavior, as suggested to occur for ions with a high number of DOF by Schlag et al. [42] cannot be excluded. In a forthcoming publication the internal energies for fragmentation on the time scale of the SID experiments will be determined by RRKM model calculations, and compared to fragmentation energies determined from the experimental data.

From Figure 3 it is seen that the measured E_{chr} does not depend on the charge state for these dendrimer ions. In general, E_{chr} can be determined with a reproducibility of 1–2 eV (see also [43]) because of statistical variations in the data. Additionally, there can be systematic, charge dependent errors in the measured E_{chr}. First, the higher the charge state of the ions the more internal energy they can gain by activation in the nozzle–skimmer region. Consequently, less SID collision energy is needed for the multiply charged ions to have the same internal energy as a lower charge state. Hence there can be a systematic underestimation of E_{chr}

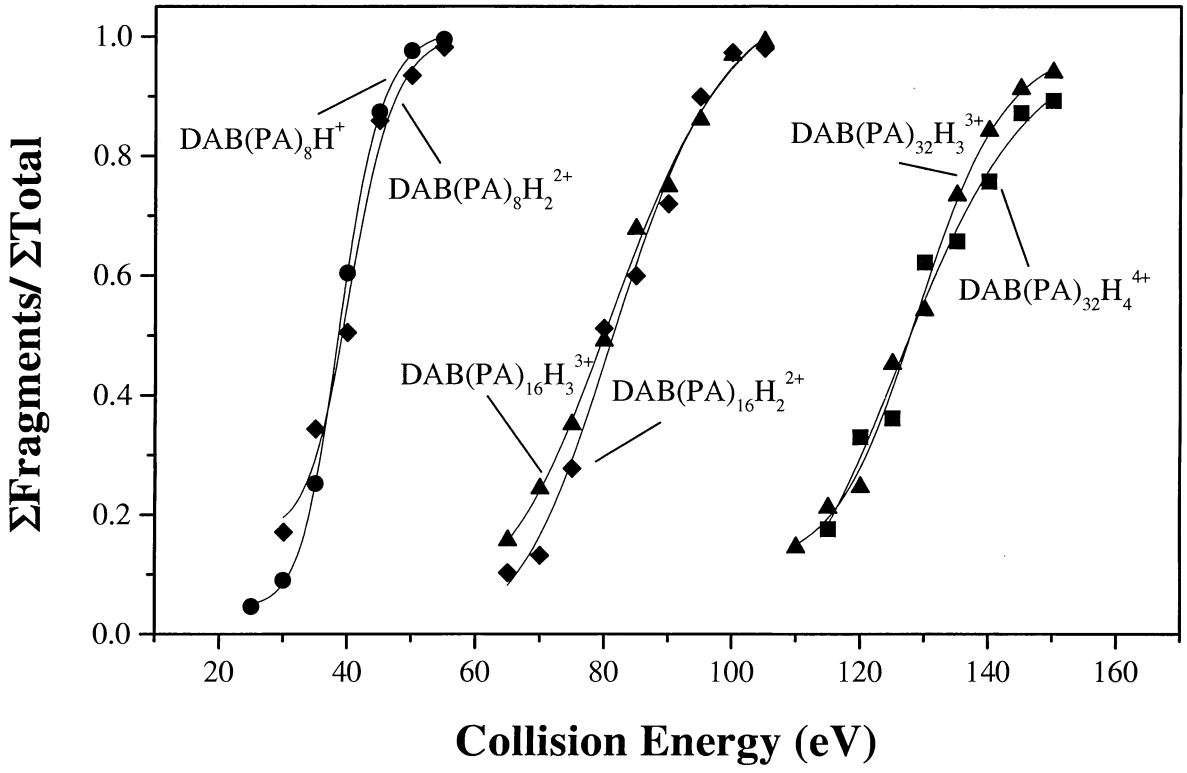

Figure 3. Fragmentation efficiency curves of various charge states of POPAM dendrimers upon collisions with a FC_{10} surface.

for a higher charge state. A second systematic error comes from the fact that a multiply charged parent ion can give more than one charged fragment per unimolecular dissociation. Consequently, at a comparable fragmentation rate, the multiply charged ion can give a higher fragment ion abundance compared to a singly charged ion. This could also introduce a shift in E_{chr} to lower values for the higher charge states. Thus, although the experimental values of E_{chr} are charge state independent, a small increase in the characteristic activation energy with charge state might be present.

The charge-state independent E_{chr} of POPAM dendrimers contrasts with the results for protonated peptides, for which lower E_{chr} have been observed for higher charge states [12, 13]. This contrast can be explained in terms of the "mobile proton" model for the fragmentation of protonated peptides. As described in the previous section, the probability of protonation of the sites at which the S_Ni fragmentation occurs is high at low internal energies for the charge states of the POPAM dendrimers used in this study. Hence it is not necessary to "mobilize" protons to cause fragmentation, and therefore there is no benefit of multiple charging. The observed independence of E_{chr} on the charge state of protonated POPAM dendrimers also suggests that there is no significant destabilization by Coulomb repulsion within the multiply charged ions selected for activation. Experiments with higher charge states would be interesting because stronger Coulomb effects may affect the fragmentation efficiency more distinctly. Larger destabilizing effects for sufficiently high charge states might lead to an observable decrease of E_{chr}. Alternatively, a higher activation energy for the S_Ni fragmentation of higher charge states may be required, when the charges are driven to primary amine sites (N-1) by Coulomb repulsion. However, we have not been able to obtain sufficient highly charged dendrimers in our ESI source to test this hypothesis. In this case additional activation energy may be needed, to mobilize the protons to the tertiary sites (N-2 and N-3), which could increase E_{chr}.

Table 2. The collision energy values at the inflection points of the fragmentation efficiency curves (characteristic collision energy, E_{chr}) for the investigated POPAM dendrimers

Parent ion	E_{chr} (eV)	Number of DOF
$DAB(PA)_8H^+$	39.0	447
$DAB(PA)_8H_2^{2+}$	40.7	450
$DAB(PA)_{16}H_2^{2+}$	82.6	966
$DAB(PA)_{16}H_3^{3+}$	82.7	969
$DAB(PA)_{32}H_3^{3+}$	129.4	2121
$DAB(PA)_{32}H_4^{4+}$	127.3	2124

Conclusions

The origin of most of the fragment ions from singly and multiply protonated POPAM dendrimers can be explained based on charge-directed S_Ni reactions. Ob-

served trends in relative abundances of fragments for different charge states of the dendrimers can be explained based on competition between minimization of the Coulomb repulsion and proton occupation of the sites with the highest gas phase basicities.

The characteristic fragmentation energy is found to increase with the size of the dendrimers. However, in contrast to previous results for multiply protonated peptides of comparable size and charge states, no dependence of the characteristic fragmentation energy on the charge state of the POPAM dendrimers is observed. Apparently, for the charge states produced in the ESI source, Coulomb forces due to multiple protonation do not lead to sufficient bond weakening to influence the ease of fragmentation. The charge-state independence of the fragmentation efficiency is in contrast with previous results for multiply protonated peptides. In the protonated dendrimers, S_Ni fragmentation reactions are possible from almost any positioning of the protons. Hence proton transfers do not result in significant decrease in the activation energy of the S_Ni processes, and therefore increasing the charge state does not result in easier fragmentation. This is a characteristic difference between protonated dendrimers and protonated peptides: for the latter ions the mobilization of proton(s) from more basic sites to amide nitrogens leads to a significant decrease in the dissociation energy of the amide bond.

Acknowledgments

The authors would like to thank N. M. M. Nibbering and K. Vékey for helpful discussions. This work is performed in collaboration with the Netherlands Foundation for Research on Matter (FOM) with the support (in part) of the Netherlands Technology Foundation (STW). Support of the work at University of Arizona by the National Science Foundation, Grant CHE 9224719, and the National Institute of Health, Grant R01GM51387, is gratefully acknowledged.

References

1. Dole, M.; Mack, L. L.; Hines, R. L.; Mobley, R. C.; Ferguson, L. D.; Alice, M. B. Molecular beams of macroions. *Chem. Phys.* **1968,** *49*, 2240–2249.
2. Yamashita, M.; Fenn, J. B. Electrospray ion source. Another variation on the free jet theme. *J. Phys. Chem.* **1984,** *88*, 4451–4459.
3. Barinaga, C. J.; Edmonds, C. G.; Udseth, H. R.; Smith, R. D. Sequence determination of multiply charged peptide molecular ions by electrospray ionization tandem mass spectrometry. *Rapid Commun. Mass Spectrom.* **1989,** *3*, 160–164.
4. Hunt, D. F.; Henderson, R. A.; Shabanowitz, J.; Sakaguchi, K.; Michel, H.; Sevilir, N.; Cox, A. L.; Apella, E.; Engelhard, V. H. Characterization of peptides bound to the Class I MHC molecule HLA-A2.1 by mass spectrometry. *Science* **1992,** *255*, 1261–1263.
5. O'Connor, P. B.; Speir, J. P.; Senko, M. W.; Little, D. P.; McLafferty, F. W. Tandem mass spectrometry of carbonic anhydrase. *J. Mass Spectrom.* **1995,** *30*, 88–93.
6. Loo, J. A.; Edmonds, C. G.; Smith, R. D. Tandem mass spectrometry of very large molecules: serum albumin sequence information from multiply charged ions formed by electrospray ionization. *Anal. Chem.* **1991,** *63*, 2488–2499.
7. Smith, R. D.; Barinaga, C. J. Internal energy effects in the collision-induced dissociation of large biopolymer molecular ions produced by electrospray ionization tandem mass spectrometry of cytochrome c. *Rapid Commun. Mass Spectrom.* **1990,** *4*, 54–57.
8. Senko, M. W.; Speir, J. P.; McLafferty, F. W. Collisional activation of large multiply charged ions using Fourier transform mass spectrometry. *Anal. Chem.* **1994,** *66*, 2801–2808.
9. Burlet, O.; Orkiszewski, R. S.; Ballard, K. D.; Gaskell, S. J. Charge promotion of low-energy fragmentations of peptide ions. *Rapid Commun. Mass Spectrom.* **1992,** *6*, 658–662.
10. Tang, X.-J.; Thibault, P.; Boyd, R. K. Fragmentation reactions of multiply protonated peptides and implications for sequencing by tandem mass spectrometry with low-energy collision induced dissociation. *Anal. Chem.* **1993,** *65*, 2824–2834.
11. Jones, J. L.; Dongré, A. R.; Somogyi, Á.; Wysocki, V. H. Sequence dependence of peptide fragmentation efficiency curves determined by ESI/SID MS. *J. Am. Chem. Soc.* **1994,** *116*, 8368–8369.
12. Dongré, A. R.; Somogyi, Á.; Wysocki, V. H. Surface-induced dissociation: an effective tool to probe structure, energetics and fragmentation mechanisms of protonated peptides. *J. Mass Spectrom.* **1996,** *31*, 339–350.
13. Dongré, A. R.; Jones, J. L.; Somogyi, Á.; Wysocki, V. H. Influence of peptide composition, gas-phase basicity, and chemical modification on fragmentation efficiency: evidence for the mobile proton model. *J. Am. Chem. Soc.* **1996,** *118*, 8365–8374.
14. Nair, H.; Somogyi, Á.; Wysocki, V. H. Effect of alkyl substitution at the amide nitrogen on amide bond cleavage: electrospray ionization/surface-induced dissociation fragmentation of Substance P and two alkylated analogs. *J. Mass Spectrom.* **1996,** *31*, 1141–1148.
15. Smith, R. D.; Loo, J. A.; Barinaga, C. J.; Edmonds, C. G.; Udseth, H. R. Collisional activation and collision-activated dissociation of large multiply charged polypeptides and proteins produced by electrospray ionization. *J. Am. Soc. Mass Spectrom.* **1990,** *1*, 53–65.
16. Jockush, R. A.; Schnier, P. D.; Price, W. D.; Strittmatter, E. F.; Demirev, P. A.; Williams, E. R. Effects of charge state on fragmentation pathways, dynamics and activation energies of ubiquitin ions measured by BIRD. *Anal. Chem.* **1997,** *69*, 1119–1126.
17. Cox, K. A.; Gaskell, S. J.; Morris, M.; Whiting, A. Role of the site of protonation in the low-energy decompositions of gas-phase peptide ions. *J. Am. Soc. Mass Spectrom.* **1996,** *7*, 522–531.
18. McCormack, A. L.; Somogyi, Á.; Dongré, A. R.; Wysocki, V. H. Fragmentation of protonated peptides: surface-induced dissociation in conjunction with a quantum mechanical approach. *Anal. Chem.* **1993,** *65*, 2859–2872.
19. Somogyi, Á.; Wysocki, V. H.; Mayer, I. The effect of protonation site on bond strengths in simple peptides: application of ab initio and MNDO bond orders and MNDO energy partitioning. *J. Am. Soc. Mass Spectrom.* **1994,** *5*, 704–717.
20. Yalcin, T.; Csizmadia, I. G.; Peterson, M. R.; Harrison, A. G. The structure and fragmentation of B_n ($n \geq 3$) ions in peptide spectra. *J. Am. Soc. Mass Spectrom.* **1996,** *7*, 233–242.
21. Rockwood, A. L.; Busman, M.; Smith, R. D. Coulombic effects in the dissociation of large highly charged ions. *Int. J. Mass Spectrom. Ion Processes* **1991,** *111*, 103–129.
22. Vékey, K.; Gömöry, Á. Theoretical modelling of mass spectrometric behaviour of peptides: singly and doubly protonated glycine. *Rapid Commun. Mass Spectrom.* **1996,** *10*, 1485–1496.
23. Mengerink, Y.; Mure, M.; Brabander, E. M. M. d.; Wal, S. v. d. Exclusion chromatochraphy of polypropylenamine dendrimers. *J. Chrom. A* **1996,** *730*, 75–81.
24. Yamdagni, R.; Kebarle, P. Gas-phase basicities of amines.

Hydrogen bonding in proton-bound amine dimers and proton-induced cyclization of α,ω-diamines. *J. Am. Chem. Soc.* **1973,** *95*, 3504–3510.
25. Whitney, T. A.; Klemann, L. P.; Field, F. H. Investigation of polytertiary alkylamines using chemical ionization mass spectrometry. *Anal. Chem.* **1971,** *43*, 1048–1052.
26. Weener, J. W.; Van Dongen, J. L. J.; Hummelen, J. C.; Meijer, E. W. Fragmentation studies of poly(propylene imine) dendrimers in the gas-phase by using electrospray ionization mass spectrometry (ESI-MS). *Polym. Mater. Sci. Eng.* **1997,** *77*, 147–148.
27. de Maaijer-Gielbert, J.; Gu, C. G.; Somogyi, Á.; Wysocki, V. H.; Kistemaker, P. G.; Weeding, T. L. ESI/SID of POPAM dendrimers. *Adv. Mass Spectrom.* **1998,** *14*, CD-ROM ThOR09.
28. Cooks, R. G.; Ast, T.; Mabud, M. A. Collisions of polyatomic ions with surfaces. *Int. J. Mass Spectrom. Ion Processes* **1990,** *100*, 209–265.
29. Vékey, K.; Somogyi, Á.; Wysocki, V. H. Internal energy distribution of benzene molecular ion in surface-induced dissociation. *J. Mass Spectrom.* **1995,** *30*, 212–217.
30. de Maaijer-Gielbert, J.; Somogyi, Á.; Wysocki, V. H.; Kistemaker, P. G.; Weeding, T. L. Surface-induced dissociation of diphenyl ether. *Int. J. Mass Spectrom. Ion Processes* **1997,** *174*, 81–94.
31. Wysocki, V. H.; Ding, J.-M.; Jones, J. L.; Callahan, J. H.; King, F. L. Surface-induced dissociation in tandem quadrupole mass spectrometers: a comparison of three designs. *J. Am. Soc. Mass Spectrom.* **1992,** *3*, 27–32.
32. Bier, M. E.; Amy, J. W.; Cooks, R. G.; Syka, J. E. P.; Ceja, P.; Stafford, G. A tandem quadrupole mass spectrometer for the study of surface-induced dissociation. *Int. J. Mass Spectrom. Ion Processes* **1987,** *77*, 31–47.
33. Chowdhury, S. K.; Katta, V.; Chait, B. T. An electrospray-ionization mass spectrometer with new features. *Rapid Commun. Mass Spectrom.* **1990,** *4*, 81–87.
34. Papac, D. I.; Schey, K. L.; Knapp, D. R. Combination electrospray-liquid secondary ion mass spectrometry ion source. *Anal. Chem.* **1991,** *63*, 1658–1660.
35. de Maaijer, J.; Heeren, R. M.; Drahos, L.; Vékey, K.; Kistemaker, P. G.; Weeding, T. L., in preparation.
36. Lias, S. G.; Bartmess, J. E.; Liebman, J. F.; Holmes, J. L.; Levin, R. D.; Mallard, W. G. Gas-phase ion and neutral thermochemistry. *J. Phys. Chem. Ref. Data* **1988,** *17*, Suppl. 1.
37. Meot-Ner (Mautner), M.; Hamlet, P.; Hunter, E. P.; Field, F. H. Internal and external solvation of polyfunctional ions. *J. Am. Chem. Soc.* **1980,** *102*, 6393–6399.
38. Schnier, P. D.; Gross, D. S.; Williams, E. R. On the maximum charge state and proton transfer reactivity of peptide and protein ions formed by electrospray ionization. *J. Am. Soc. Mass Spectrom.* **1995,** *6*, 1086–1097.
39. Schnier, P. D.; Price, W. D.; Williams, E. R. Modeling the maximum charge state of arginine-containing peptide ions formed by electrospray ionization. *J. Am. Soc. Mass Spectrom.* **1996,** *7*, 972–976.
40. Meot-Ner (Mautner), M.; Dongré, A. R.; Somogyi, Á.; Wysocki, V. H. Thermal decomposition kinetics of protonated peptides and peptide dimers, and comparison with surface-induced dissociation. *Rapid Commun. Mass Spectrom.* **1995,** *9*, 829–836.
41. Beck, R. D.; Rockenberger, J.; Weis, P.; Kappes, M. M. Fragmentation of C_{60}^+ and higher fullerenes by surface impact. *J. Chem. Phys.* **1996,** *104*, 3638–3650.
42. Schlag, E. W.; Levine, R. D. On the unimolecular dissociation of large molecules. *Chem. Phys. Lett.* **1989,** *163*, 523–530.
43. Vékey, K.; Somogyi, Á.; Wysocki, V. H. Average activation energies of low-energy fragmentation processes of protonated peptides determined by a new approach. *Rapid Commun. Mass Spectrom.* **1996,** *10*, 911–918.